

Thermal radiant exitance model performance: soils and forests

Lee K. Balick

EG&G Energy Measurements Inc.
Mail Stop RSL-19, P.O. Box 1912
Las Vegas, Nevada, USA 89125

James A. Smith

Laboratory for Terrestrial Physics
NASA Goddard Space Flight Center
Greenbelt, Maryland, USA 20771

ABSTRACT

Models of surface temperatures of two land surface types based on their energy budgets were developed to simulate the effects of environmental factors on thermal radiant exitance. The performance of these models is examined in detail.

One model solves the non-linear differential equation for heat diffusion in solids using a set of submodels for surface energy budget components. The model performance is examined under three desert conditions thought to be a strong test of the submodels. The accuracy of the temperature predictions and submodels is described. The accuracy of the model is generally good but some discrepancies between some of the submodels and measurements are noted. The sensitivity of the submodels is examined and is seen to be strongly controlled by interaction and feedback among energy components that are a function of surface temperature.

The second model simulates vegetation canopies with detailed effects of surface geometry on radiant transfer in the canopy. Foliage solar absorption coefficients are calculated using a radiosity approach for a three layer canopy and long wave fluxes are modeled using a view factor matrix. Sensible and latent heat transfer through the canopy are also simulated using nearby meteorological data but heat storage in the canopy is not included. Simulations for a coniferous forest canopy are presented and the sensitivity of the model to environmental inputs is discussed.

1. INTRODUCTION

This paper describes the performance of two models to simulate the apparent terrain temperatures of soil and vegetation. Tests of the soil surface temperature models were made at desert sites in the southwestern United States and the vegetation model was tested for a northern coniferous forest site in the state of Maine.

2. SOIL MODEL2.1 Purpose of the model

The model used to simulate soil temperatures was developed as one of a small set of temperature models for two main objectives: examining the effects of the environment on the thermal infrared signatures of target backgrounds and to provide reasonable estimates of radiant exitance of flat, solid scene components for image modeling. Solid scene components include constructed materials such as roads and runways as well as soils. Therefore, choices were made to maximize the generality and flexibility of the model while minimizing the input requirements (especially those data that are difficult to obtain).

2.2 The model and model structure

Like several similar models, this model¹ solves the one dimensional nonlinear differential equation for heat conduction in solids and determines surface temperatures through the evaluation of the upper boundary conditions. The generic quality of the model allows its performance to be pertinent to several related models which have been used for generally similar applications^{2,3,4,5}.

MASTER *ds*
DISTRIBUTION OF THIS DOCUMENT IS UNLIMITED

DISCLAIMER

**Portions of this document may be illegible
in electronic image products. Images are
produced from the best available original
document.**

The structure of the model facilitates changing the level of detail and input requirements for the surface-atmosphere interactions by using submodels for each of these energy exchange mechanisms: solar energy absorption (S), thermal (infrared) energy absorption (R_{down}), thermal emission (R_{up}), sensible heat transfer (H), and latent heat transfer (L). The simulation of heat conduction (C) from the surface into the ground is more fixed because it is integrated into the numerical solution. In this model, heat is conducted through layers which have vertically and temporally (and horizontally) uniform properties specified by heat conductivity and thermal diffusivity. Continuous profiles of vertically varying soil properties are approximated by varying layer properties. At the surface-atmosphere boundary the sum of the six energy fluxes is zero so that the surface temperature is the temperature which satisfies this requirement. Because several of these components depend on surface temperature, the model contains several feedback paths which will be seen to strongly affect model performance. The air-surface boundary condition is evaluated using these energy flux components while the bottom boundary condition (usually a fixed temperature) and an initial condition must be specified.

More rigorously, the one-dimensional nonlinear differential equation for heat transfer in solids, Equation 1, is solved using

$$\frac{\partial T(z, t)}{\partial t} = \alpha(z) \frac{\partial^2 T(z, t)}{\partial z^2} \quad (1)$$

where T is temperature, t is time, z is the depth in the soil layer, and α is the thermal diffusivity of the soil. Equation 1 is solved using a simple explicit finite difference scheme for an arbitrary number of uniform layers. At the upper boundary, the energy components sum to zero so the surface temperature that satisfies this condition is found using a Newton-Raphson iteration scheme. However, it is from the solution to the upper boundary value, or the surface energy budget, that the surface temperature is derived and where the environmental controls are incorporated into the simulation. The focus of this work is on the simulation of the surface energy budget.

The surface energy budget is estimated using a submodel for each of the energy budget components. These may be modified as necessary to adapt to the requirements of the simulation and data availability but for clarity in this work, and for most operational simulation contexts, fairly simple forms of the submodel are used. For the solar energy entering the system, the submodel is simply

$$S = (1 - a) * S_i \quad (2)$$

where a is the albedo and S_i is the irradiance. As a practical matter, S_i is often measured and can be well simulated, at least for clear sky conditions. Similarly, for the longwave or thermal IR energy entering the system

$$R_{down} = \varepsilon_s * R_i \quad (3)$$

where ε_s is the graybody emissivity of the surface and R_i is the longwave irradiance. R_i can be measured but is estimated here with Brunt equation modified for cloud cover^{1,6,7}:

$$R_{down} = \sigma T_a^4 * (c + b(e_a^s)) * (1 + CIR * CC^2) \quad (4)$$

where σ is the Stephan-Boltzman constant, b and c are constants. T_a is the air temperature, e_a is the water vapor pressure of the atmosphere near the surface, CIR is an empirical coefficient depending on cloud type, and CC is the portion of sky cover. Thermal energy leaving the system is proportional to the estimated surface temperature:

$$R_{up} = \varepsilon_s \sigma T_s^4 \quad (5)$$

where ε_s is the emissivity of the surface material, and T_s is the estimated surface temperature. The turbulent heat fluxes, sensible heat (H) and latent heat (L) are modeled with the aerodynamic approach following Oke⁷:

$$\begin{aligned} H &= -\rho c_p \kappa^2 Z^2 \left(\frac{\partial u}{\partial Z} \right) \left(\frac{\partial \Theta}{\partial Z} \right) SCF \quad \text{and} \\ L &= -\rho l \kappa^2 Z^2 \left(\frac{\partial u}{\partial Z} \right) \left(\frac{W \partial q}{\partial Z} \right) SCF \end{aligned} \quad (6)$$

where ρ is the air density near the ground, c_p is the specific heat of dry air at constant pressure. κ is von Karman's constant, Z is the measurement height above the surface, $\partial \Theta / \partial Z$, $\partial u / \partial Z$, and $\partial q / \partial Z$ are the gradient of the potential temperature

and wind speed and specific humidity of air near the surface, SCF is an adjustment factor for atmospheric stability which is a function of the Richardson's number, l is the latent heat of evaporation, and W is an empirical factor related to soil saturation used to account for moist but unsaturated conditions. Finally, heat conduction into the soil is defined as:

$$C = -K \left(\frac{\partial T}{\partial z} \right) \quad (7)$$

where K is the heat conductivity of soil near the surface and $(\partial T / \partial z)$ is the gradient of soil temperature between the surface and the first grid point below the surface.

Since there are several choices possible for each of the energy budget submodels, the performance of the model is evaluated against the submodels instead of input measurements and specifications. (The sensitivity of this model to inputs is described in Balick et. al.¹ and excellent descriptions of the sensitivity to inputs in related models to inputs can be found in Hughes et. al.⁴.) Some attention will be given to evaluating the validity of the submodels and their interactions. The sensitivity of the model and submodel interactions to changes of individual submodel results will also be examined.

2.3 Soil model performance

2.31 Accuracy

Figures 1a and 1b show comparisons of model estimates against hand-held radiometer measurements for two desert conditions. In both cases, the thermal properties of the soil were not measured so the model was "tuned" to reasonable approximations of soil thermal properties so it is not fully valid to take these results as an evaluation of accuracy. They are presented to show that the model is reasonable and as a baseline for the results to follow. For both sets of conditions, the thermal properties found this way were quite plausible. Figure 1a is from data from a dry sand flat near Moab, Utah near the summer solstice. The site had very low heat conductivity and very strong solar irradiance: a time and place chosen to stress the turbulent heat transfer submodels. The model accuracy was quite reasonable (although the thermal properties were derived from the same data). Both the model and the measurements show very strong heating - over 50C during the day. Figure 1b shows similar data from a site near Tucson, Arizona in September. Both the atmospheric and soil conditions were more moderate than the Moab case. Again, the model estimates are quite reasonable (although, again, this is somewhat of a circular logic).

2.32 Submodel validation

Of particular interest for validation are the submodels for the sensible and latent heat transfers and the longwave inputs. Solar energy input was measured and models are usually reliable, longwave exitance is, essentially, the answer, and heat conduction was not measured well in these field conditions. The validity of individual submodels affects other submodels that depend on the surface temperature through feedback in the model and these effects will be shown. (Due to time and space limitations, only results from one day at Tucson are presented. The full analyses were performed on the Moab case and two days at Tucson. There are some differences - but no surprises - and the case to be shown is representative.) Independent determination of sensible and latent heat components were acquired by Dr. Lloyd Gay at the University of Arizona using a carefully calibrated Bowen Ratio measurement system.

Figure 2 shows the model results when measurements of H are substituted for the submodel results. Shown in this figure are the estimated T_s , the R_{up} , L , H , and C at the surface from 05:30 to 24:00 MST (except the surface temperatures, all are energy flux densities in W/m^2) with and without the substitution. The measured sensible heat fluctuated more than the model estimates during the day and the model tended to overestimate the magnitude of H by 20-30 W/m^2 during the middle of the day. To a degree, this was compensated by a change of C and L so that the net effect on the T_s was less than a degree when measurements of the H were used in lieu of the submodel. While the latent heat flux calculations did not change much, they were not very accurate. Figure 3 shows that the estimates of L from the submodel significantly underestimated this component. Compensation occurred in both H and C components so that the T_s estimates did not change more than 2C. This tendency to compensate for errors through feedback loops is a strong characteristic of the model performance. When measurements of H , L and R_{down} are all substituted for submodels, some of the feedback paths are cut off and only the heat conduction component can change. This is shown in Figure 4 where temperature changes around 3C, up to 4C are observed in the morning and afternoon. The temperature estimate changes and the differences of the conduction component are closely correlated.

2.33 Sensitivity to submodels

Figure 5 shows the results of varying the sensible heat flux submodel by a factor of two. Because of feedbacks, the realized difference of estimates of H was considerably less than a factor of two and the resulting change of simulated T_s was around 2C in the middle of the day, less at other times. Changing the latent heat submodel by a factor of two, shown in Figure 6, results in smaller changes of T_s than for sensible heat because the size of the term is much smaller. In Figure 7, the longwave energy flux input to the system is modified by factors of 0.5, 1.5, and 2.0. For any of these, the impact on the energy budget is substantially larger than for H and L . This is because the component is not a function of T_s and is not in a feedback path. While the T_s estimate changes are larger than for the turbulent transfers, submodels are usually more precise, as we saw in validation case presented earlier. Calculations were performed with the heat conductivity of the top 10 cm of soil at its original value of 0.05 cal/cm-min-K and with it changed to 0.02 and 0.10 cal/cm-min-K. T_s estimates changed by 2C or more during the day and by nearly the same amount but the opposite direction at night: there is about a 5C change in the range of temperatures estimated. At night, feedback through the turbulent transfer components is damped.

3. FOREST MODEL

3.1 Purpose of the model

The use of thermal scanning devices offers a potential tool for estimating evapotranspiration and latent heat flux densities in forest canopies⁸. Modeling underlying energy exchanges is necessary, however, in order to fully capitalize on this potential. Incorporating diurnal latent and sensible heat flux terms, coupled to canopy geometry, may also be necessary in order to predict physically based texture parameters in diurnal thermal images⁹.

The model described below is much simpler than the recent model described by Koivunen¹⁰ which treats individual leaves but we use the same radiosity method to compute long-wave and short-wave flux transfers. On the other hand, our model is more complex than other recently proposed remote sensing models¹¹. Yamazaki, et al¹² have developed a heat balance model for a canopy with one or two layers.

3.2 The model and model structure

The basic thermal model abstracts a forest canopy as consisting of three vegetation layers, the sky and a ground layer, which act as both sources and sinks of thermal energy. The steady-state energy budget equations for each canopy layer may be summarized as follows¹³:

$$F_i(\mathbf{X}) = \frac{1}{2} \alpha_i \sum_j B_j S_{ij} - B_i + A_i + H_i(\mathbf{X}) + LE_i(\mathbf{X}) = 0 \quad (8)$$

where

$\mathbf{X} = (X_1, X_2, X_3, \dots)^T$ are the average layer temperatures for layers 1,2,3,...

α = the vector of long-wave absorptivities (3 to 30 micrometers) for each vegetation layer

B = the long wave emission terms from the atmosphere, canopy, and ground layers

$$\mathbf{B} = [B(T_a) \quad B(X_1) \quad B(X_2) \quad B(X_3) \quad B(T_g)] \quad (9)$$

T_a = air temperature

T_g = ground temperature

S_{ij} = the canopy configuration factor matrix which summarizes the fraction of flux from a source layer or scattering element, j , that is intercepted by a sink layer or scattering element, i , and is described in the paper by Smith and Goltz¹⁴

A = the vector of shortwave (0.4 to 3.0 micrometers) absorption flux in each canopy layer

H = the vector of sensible heat for each layer

LE = the vector of evapotranspiration terms

An iterative Newton-Raphson technique is used to solve the nonlinear thermal equations for temperature profile, \mathbf{X} :

$$\delta \mathbf{X} = (\mathbf{J}^T \mathbf{J})^{-1} \mathbf{J}^T [-\mathbf{F}(\mathbf{X}_0)]; \quad J_{ij} = \frac{\partial F_j}{\partial X_i} \quad (10)$$

where \mathbf{X}_0 is an initial guess, usually taken as, T_a , and \mathbf{J} is the Jacobian of the system.

Each of the surface energy budget terms for shortwave absorption, sensible and latent-heat, are computed using submodels which may be modified as needs and data availability dictate.

Short-wave energy absorption within the canopy-soil system is estimated using the radiosity approximation as discussed by Smith and Goltz¹⁴. The sensible heat submodel employs the standard resistance relationship using a wind speed profile calculated as a function of above canopy wind speed, the canopy displacement height, the roughness length at the soil surface, and canopy density. The formulation includes a logarithmic wind profile above the canopy and a modified exponential profile within the canopy.

Stomatal conductance is calculated from directly measured parameters following the nonlinear model of Jarvis¹⁵:

$$g_s = g_0 * f(I) * f(T) * f(\delta e) * f(\psi) \quad (11)$$

where g_s is the actual conductance, g_0 is the reference value (maximum possible conductance), $f(I)$ is a function of short wave radiation, $f(T)$ is a function of air temperature, $f(\delta e)$ is a function of the vapor pressure deficit, and $f(\psi)$ is a function of foliage water potential. These four functions vary between 0 and 1.0. The parameters used in the functions were estimated from a data set of measured stomatal conductances of spruce and hemlock and results compared with canopy resistances inferred from inversion of the Penman-Monteith equation¹⁶.

3.3 Forest model performance

3.31 Accuracy

An analysis of the basic thermal model performance was carried out at the Northern Experimental Forest study site near Howland, Maine, the location of a NASA sponsored Forest Ecosystem Dynamics Multi-sensor Aircraft Campaign¹⁷. Vegetation at the site consists of northern hardwood transitional species. Spruce was the dominant vegetation type over which measurements were performed. Energy budget data were collected under primarily clear sky conditions for a 48 hour time period beginning 2100 Local Standard Time on 2 August 1990. Sensible and latent heat-flux measurements were also obtained with eddy correlation instruments mounted 28 m above the ground and oriented towards the west. The instruments included a one-dimensional sonic anemometer with a fine-wire thermocouple and a krypton hygrometer.

Figure 8 shows a comparison of the measured and predicted canopy temperatures for the upper third of the canopy for the 48 hour diurnal cycle begun on August 2, 1990. Conditions were generally clear. The results are typical for all canopy layers which exhibited less than 1.2 degree C root mean square error with maximum error in predicted temperature of approximately 2 degrees C during peak solar heating.

3.32 Submodel validation

Figures 9 and 10 show a comparison of the modeled and measured energy balance components for sensible and latent heat respectively. Near solar noon on the second day (time period 36 on the graph), fluctuation in solar irradiance conditions occurred, resulting in additional variation in measured sensible and latent heat terms. Corresponding errors in the latent and sensible heat terms were 30 and 32 W m⁻² respectively.

3.33 Sensitivity to submodels

Several day-time sensitivity analyses were performed on the model. Predicted canopy temperatures were most sensitive to the air temperature within the canopy. A 3 degree change in canopy air temperature resulted in nearly a 3 degree change in canopy temperature. Decreasing longwave absorption coefficients by 10 percent resulted in less than a 0.5 degree Centigrade change in predicted temperatures. Predicted canopy temperatures showed less sensitivity to changes in ground temperature for this dense canopy case. A non-linear dependence of predicted canopy temperature on both stomatal resistance and wind speed was exhibited. For the conditions studied, canopy temperature varied 1-2 degrees for a variation in stomatal resistance from the nominal by a factor of three. The canopy was not under water stress.

4. SUMMARY

Soil and forest canopy thermal models have been described which incorporate diurnal sensible and latent heat terms as well as a long and short wave energy budget components. In agreement with earlier experimental comparisons, the models reported here provided reasonable estimates of scene temperatures. Reasonable estimates of sensible and latent heat flux terms for both models were also obtained for the conditions studied.

Some caveats are appropriate, however. The canopy modeled was a fully-leaved, closed canopy. Under these conditions, stems and trunks were assumed to have a minor influence on thermal transfers and were not included in the steady-state model. However, they may well have an influence for non-steady state conditions and, obviously, for leafless canopies. Similarly, mass transfer through the soil, moisture and occasionally dry air, have noticeable effects on soil surface temperatures. These effects need to be investigated. The coupling of the two models, especially for more open and less dense canopies, is also of interest.

5. ACKNOWLEDGMENTS

Prepared for the Department of Energy under Contract No. DE-AC08-93NV11265. The research described in this paper was also supported, in part, by the Remote Sensing Science Program at NASA Headquarters and by the U.S. Army Corps of Engineers Waterways Experiment Station. By acceptance of this article, the publisher and/or recipient acknowledges the U.S. Government's right to retain a nonexclusive, royalty-free license in and to any copyright covering the article. Technical assistance was provided by Mr. Randy Scoggins of the WES and manuscript preparation by Laura Rumburg of the GSC.

6. REFERENCES

1. Balick, L. K., L. E. Link, R. K. Scoggins, and J. L. Solomon, 1981. Thermal modeling of terrain surface elements, Technical Report EL-81-2, Environmental Laboratory, U. S. Army Engineer Waterways Experiment Station, Vicksburg MS.
2. Kahle, A. B., "A simple model of the earth's surface for geologic mapping by remote sensing." *Journal of Geophysical Research*, Vol 70, No. 6. pp. 1329-1337, 1977.
3. Schieldge, J. P., A. B. Kahle, and R. E. Alley, "A numerical simulation of soil temperature and moisture variations for a bare field." *Soil Science*, Vol 133., No. 4, pp 197-207. 1982.
4. Hughes, P. A., T. J. L. McComb, A. B. Rimmer, K. E. Turver, M. L. B. Rogers, A. F. Vickers, and D. W. Wright, "A mathematical model for the prediction of temperature of man-made and natural surfaces." *Int. J. Remote Sensing*, Vol 14, No. 7, pp. 1383-1412, 1993.
5. Balick, L. K., J. R. Hummel, J. A. Smith, and D. S. Kimes, 1990. One-dimensional temperature modeling techniques: review and recommendations. SWOE Report 90-1. U. S. Army Engineer Cold Regions Research and Engineering Laboratory, Hanover NH. 17 pp.
6. Sellers, W. D. 1965. Physical Climatology. University of Chicago, Chicago IL.
7. Oke, T. R., 1978, Boundary Layer Climates, Methven and Co. Lrd., Halstead Press Book, John Wiley and Sons.
8. L. L. Pierce and R. G. Congalton, "A methodology for mapping forest latent heat flux densities using remote sensing." *Remote Sens. Environ.*, vol 24. pp 405-418. 1988.
9. N. Ben-Yosef, K. Wilver, S. Sivhony, and M. Abitbol. "Correlation length of natural terrain infrared images: daily Variation." *Appl. Opt.*, vol 25. pp 866-869, 1986.
10. A. Koivunen, "A first principles heat transfer model of a deciduous tree." Proc. of the Second Annual Ground Target Modeling and Validation Conference. 20-21 August, 1991. pp. 42-55, 1991.
11. J. A. Sobrino and V. Caselles, "Thermal infrared radiance model for interpreting the directional radiometric temperature of a vegetative surface." *Remote Sens. Environ.*. vol 33, pp 193-199. 1990.

12. T. Yamazaki, J. Dondo, T. Watanbe, and T. Sato, "A heat balance model with a canopy of one or two layers and its application to field experiments." *J. Appl. Meteor.*, vol 31, pp 86-103, 1992.
13. M. J. McGuire, J. A. Smith, L. K. Balick, and B. A. Hutchison, "Modeling directional thermal radiance from a forest canopy." *Remote Sens. Environ.*, vol 27, pp 169-186, 1989.
14. J. A. Smith and S.M. Goltz, "Updated thermal model using simplified short-wave radiosity calculations." *Remote Sens. Environ.*, vol 47, pp 167-175, 1994.
15. P. G. Jarvis. "The interpretation of the variations in leaf water potential and stomatal conductance found in canopies in the field." *Philos. Trans. Roy. Soc. London B.*, vol 273, pp 593-610, 1976.
16. S. M. Goltz, L. LaCruz, F. Scott, and Z. Guan. "Surface resistance and evapotranspiration models of a spruce-fir forest." *Proc. 20th. Conf. on Agr. and Forest Meteor.*, Salt Lake City, Utah. pp 160-163, 1991.
17. J. A. Smith, K. J. Ranson, D. L. Williams, E. R. Levine, S. M. Goltz, and R. S. Katz. "A sensor fusion field experiment in forest ecosystem dynamics." *Proc. SPIE Conference on Remote Sensing of the Biosphere*, Orlando Florida, vol 1300, pp 117-132, 1990.

DISCLAIMER

This report was prepared as an account of work sponsored by an agency of the United States Government. Neither the United States Government nor any agency thereof, nor any of their employees, makes any warranty, express or implied, or assumes any legal liability or responsibility for the accuracy, completeness, or usefulness of any information, apparatus, product, or process disclosed, or represents that its use would not infringe privately owned rights. Reference herein to any specific commercial product, process, or service by trade name, trademark, manufacturer, or otherwise does not necessarily constitute or imply its endorsement, recommendation, or favoring by the United States Government or any agency thereof. The views and opinions of authors expressed herein do not necessarily state or reflect those of the United States Government or any agency thereof.

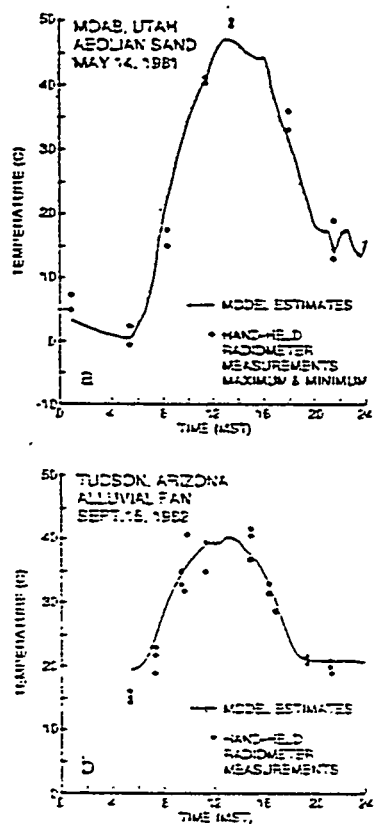


Fig. 1. Comparison of model estimates and hand-held radiometer measurements.

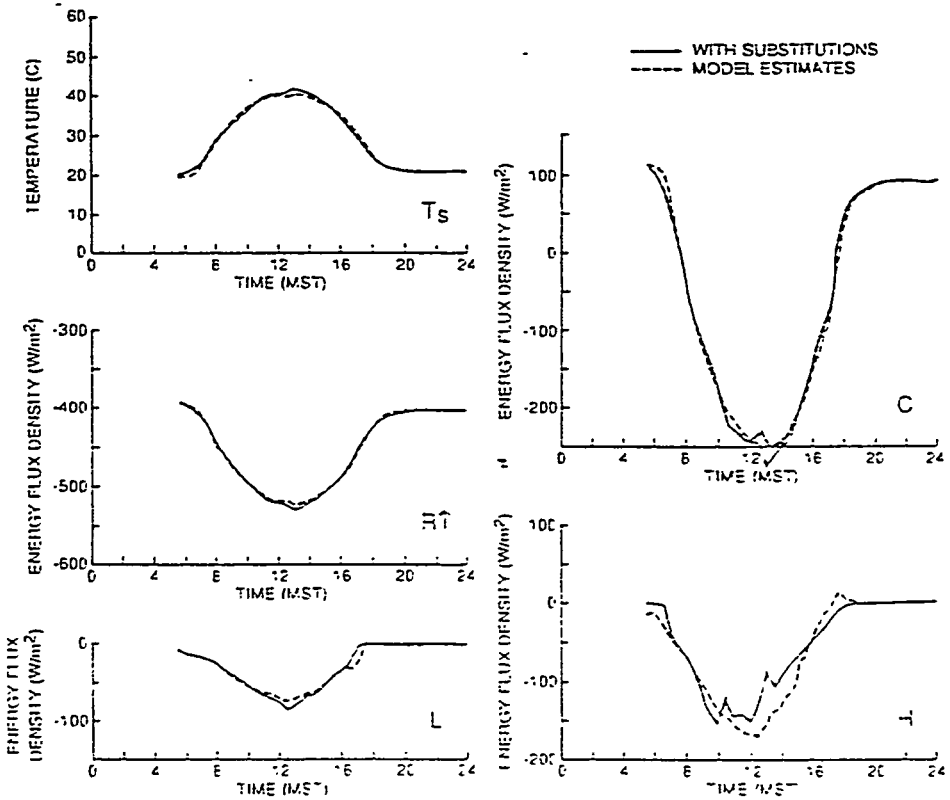


Fig. 2. Tucson, Arizona - Sensible heat measurements substituted for model estimates.

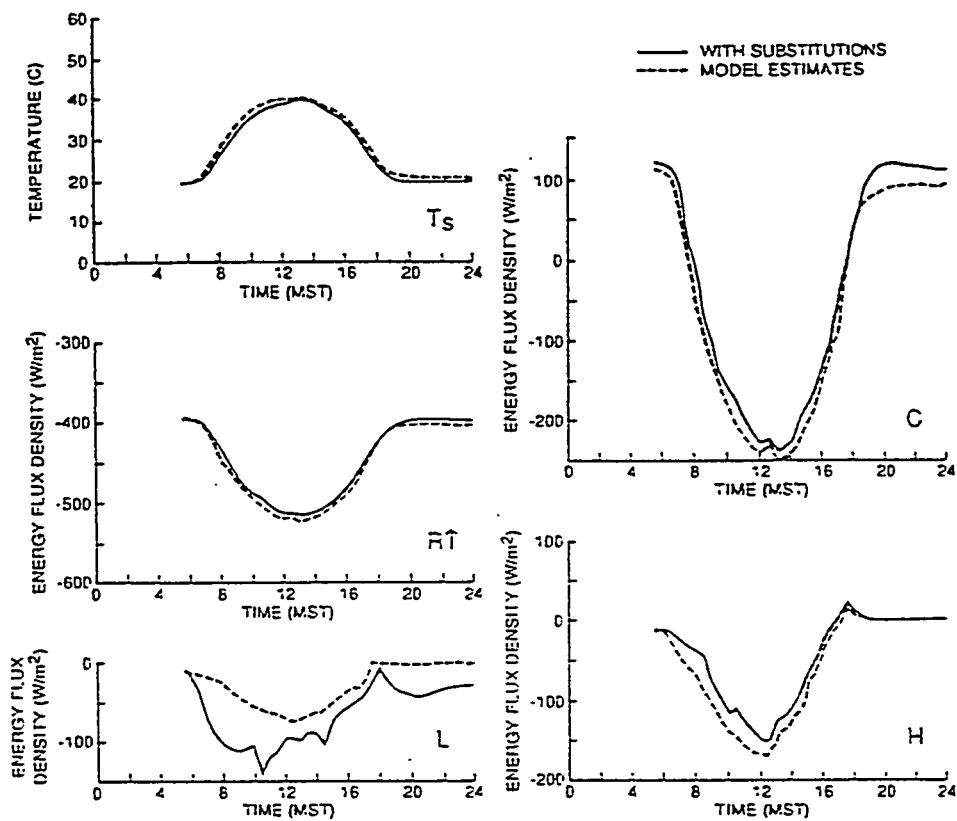


Fig. 3. Tucson, Arizona - Latent heat measurements substituted for model estimates.

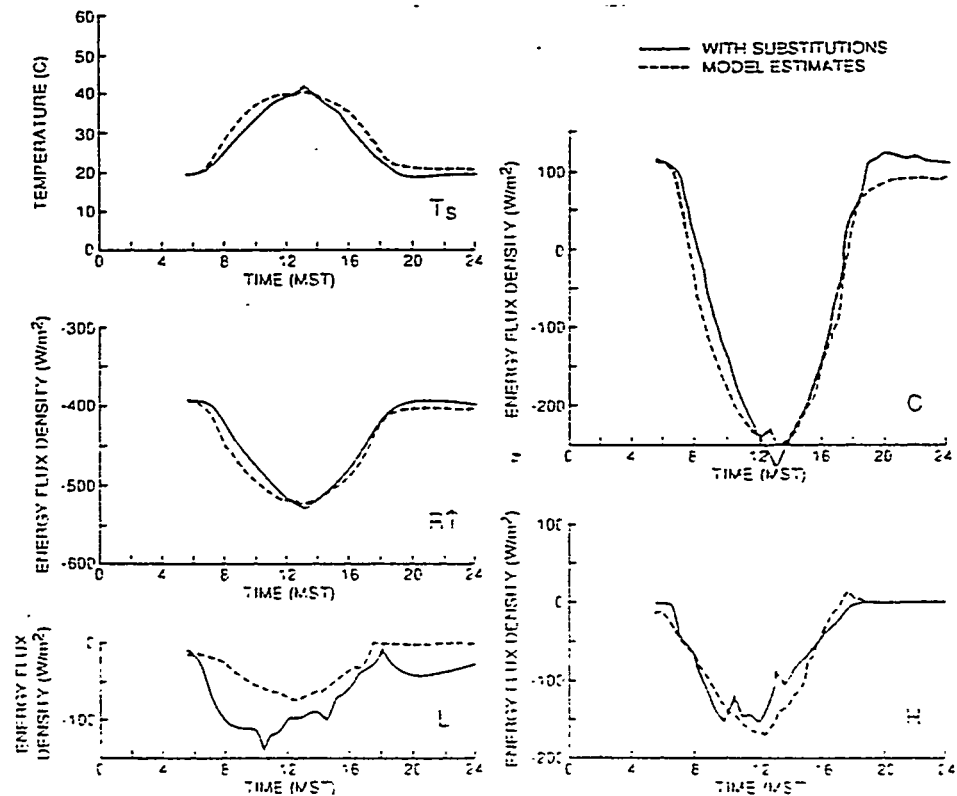


Fig. 4. Tucson, Arizona - H, L and R↓ measurements substituted for model estimates.

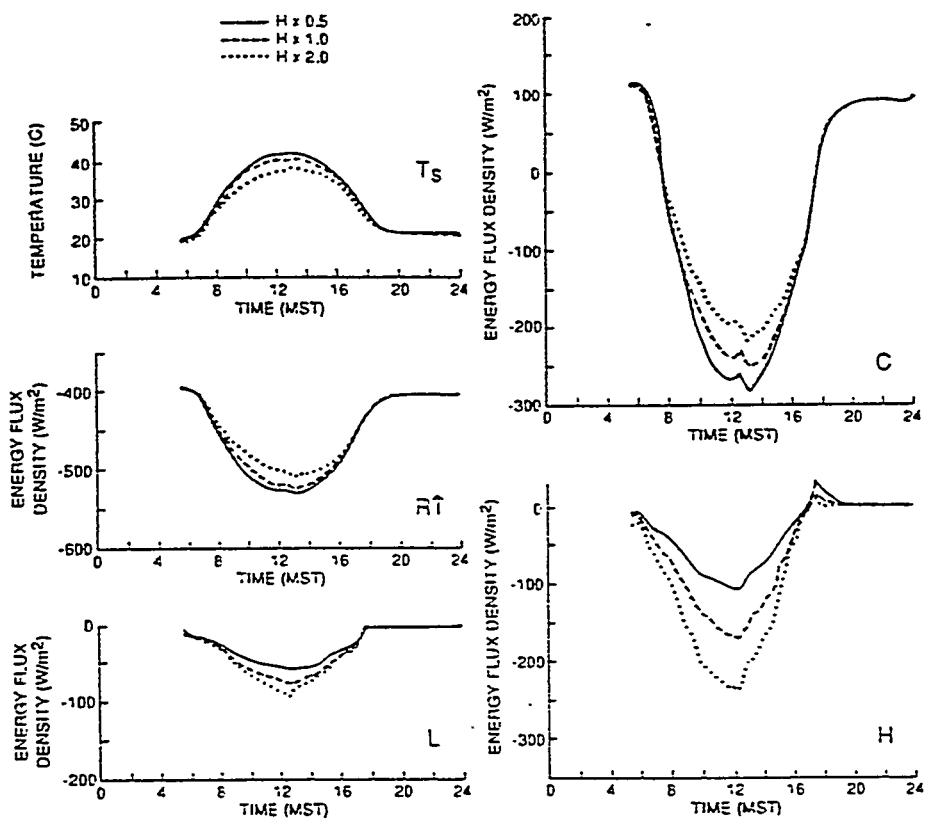


Fig. 5. Tucson, Arizona - Model sensitivity to sensible heat.

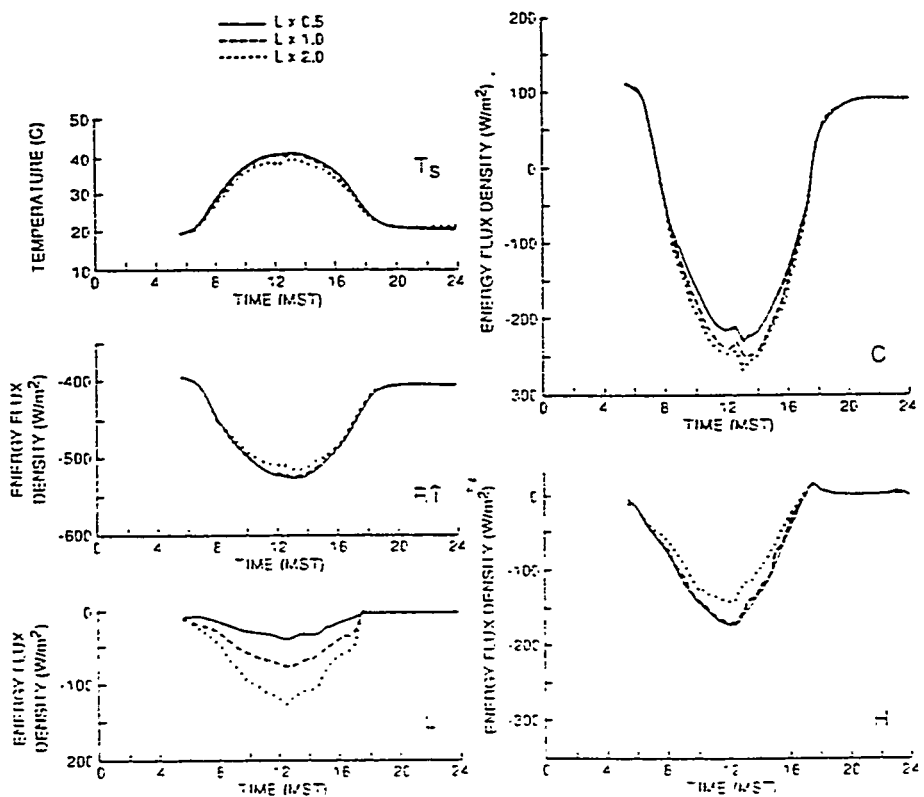


Fig. 6. Tucson, Arizona - Model sensitivity to latent heat.

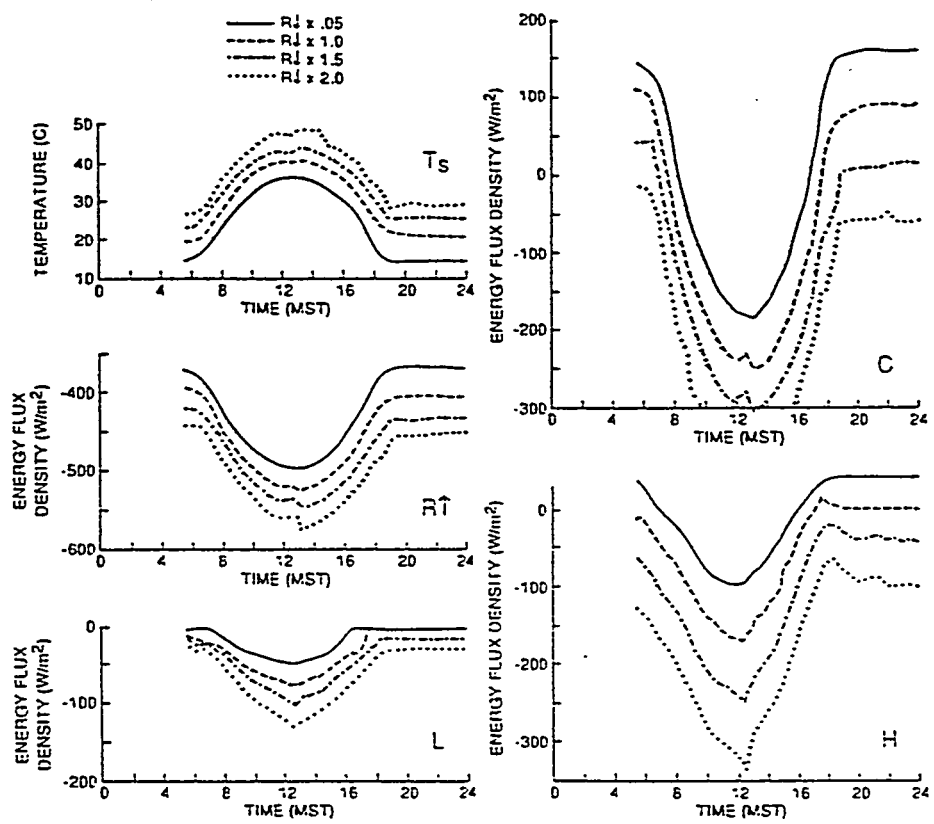


Fig. 7. Tucson, Arizona - Model sensitivity to sky thermal IR ($R\downarrow$).

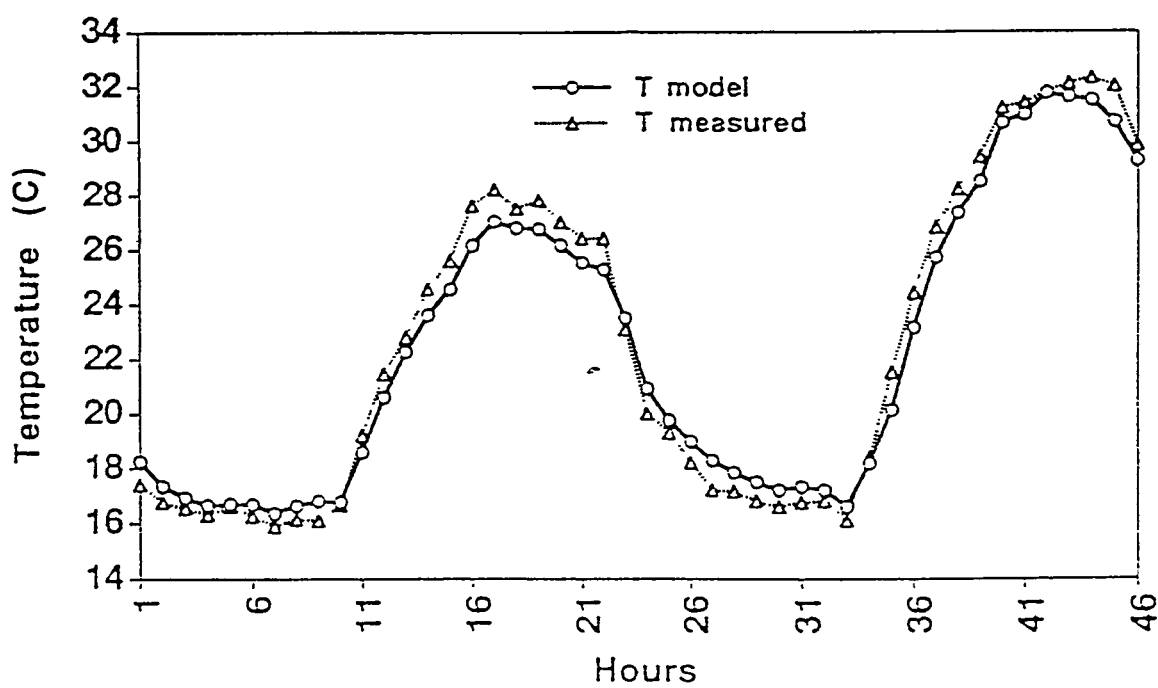


Fig. 8. Measured and modeled temperatures of upper third of canopy.

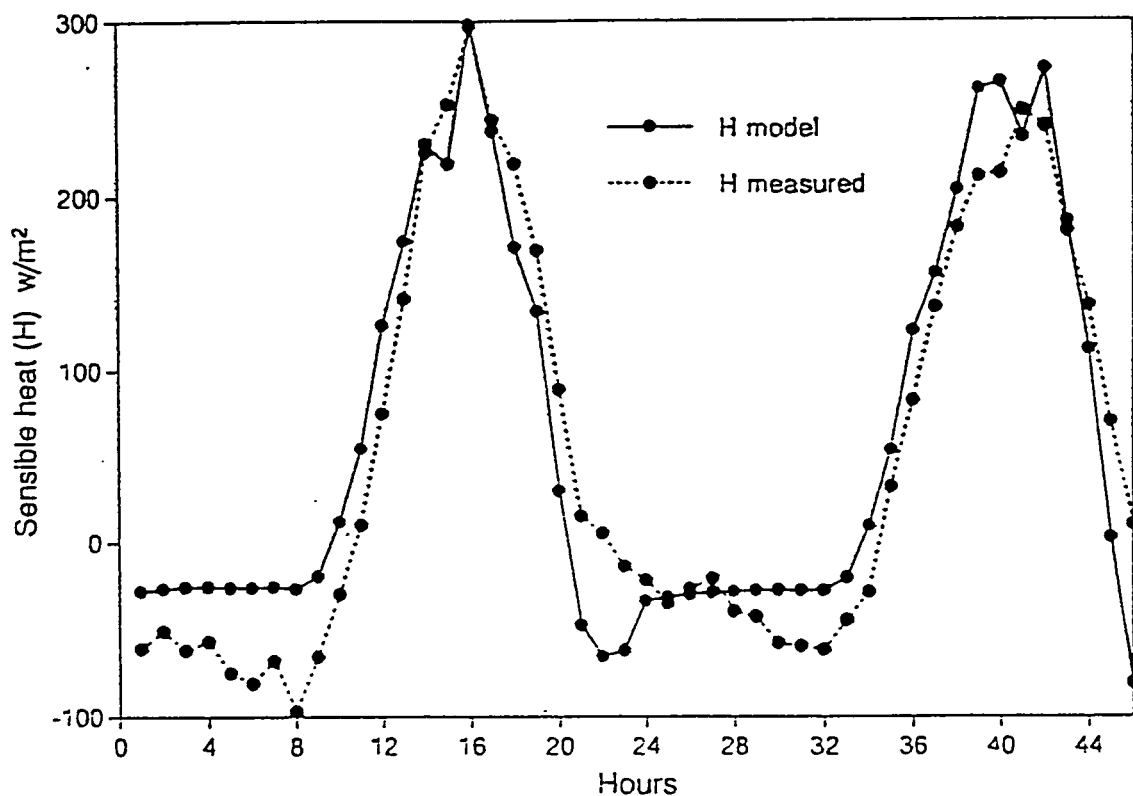


Fig. 9. Comparison of sensible heat.

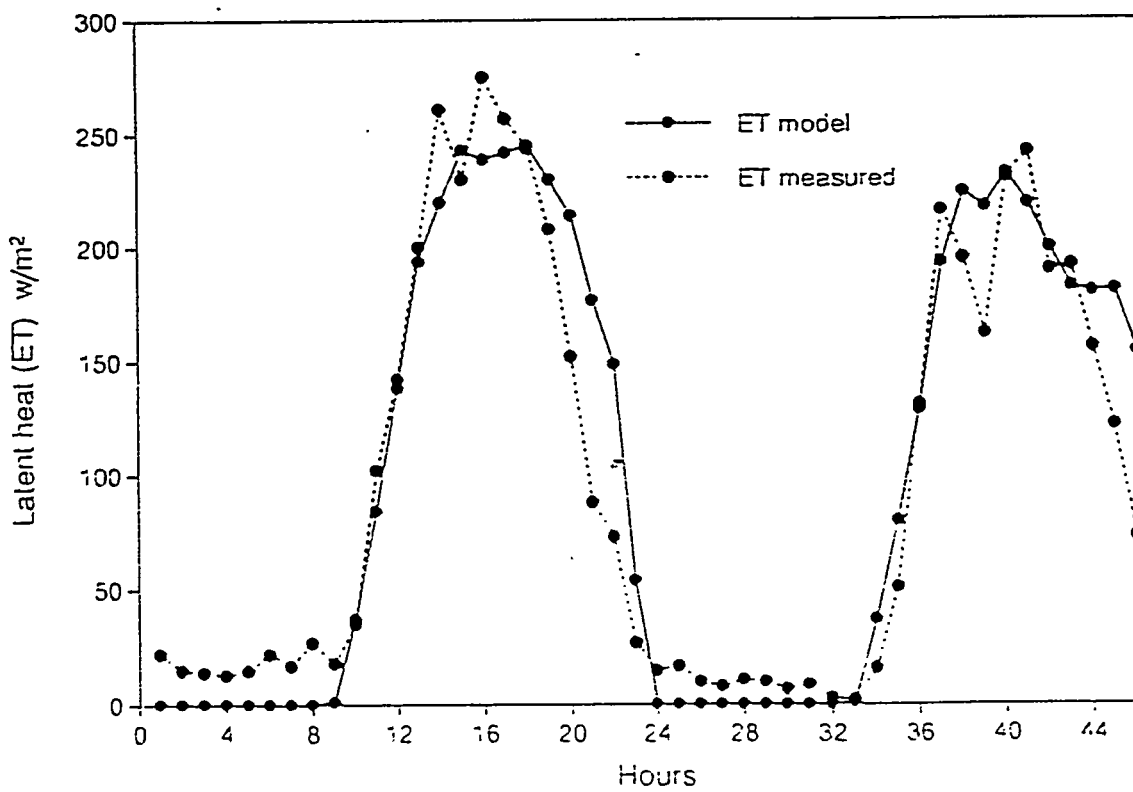


Fig. 10. Comparison of latent heat.